



## Article

# Characteristics and Drivers of Soil Organic Carbon Saturation Deficit in Karst Forests of China

Limin Zhang <sup>1,2</sup> , Yang Wang <sup>1</sup>, Jin Chen <sup>1</sup>, Ling Feng <sup>1</sup>, Fangbing Li <sup>1</sup> and Lifei Yu <sup>1,\*</sup> 

<sup>1</sup> College of Life Sciences, Guizhou University, Guiyang 550025, China; zhanglimin563406@163.com (L.Z.); wangyang20218910@126.com (Y.W.); gs.chenjin20@gzu.edu.cn (J.C.); 15870149772@163.com (L.F.); lifangbing9685@163.com (F.L.)

<sup>2</sup> Institute of Guizhou Mountain Resources, Guizhou Academy of Sciences, Guiyang 550001, China

\* Correspondence: lfyu@gzu.edu.cn

**Abstract:** Karst forests have complex and unique carbon cycle characteristics. Soil organic carbon saturation deficit (CSD) is an important indicator of soil organic carbon (SOC) sequestration potential; exploring its characteristics and driving factors is a priority theme in current research on the carbon cycles of terrestrial ecosystems. In this study, 171 topsoil samples from typical karst forests in southwest China were used as the study objects. A SOC maximum saturation capacity model was constructed using the boundary line method. The CSD is equal to the maximum saturated capacity of SOC minus the current SOC. We analyzed the CSD and its main driving factors in different regions and succession stages. The results showed that the fractions of carbon and SOC contents in the karst forests at different successional stages in descending order were as follows: climax stage > arbor stage > shrub stage > herb stage. The CSD was the highest at the herb stage in Maolan, Yuntai Mountain, and Dashahe at 83.04%, 89.99%, and 89.97%, respectively, followed by the shrub stage with 48.69%, 78.50%, and 84.95%, and the lowest at the arbor stage with 25.69%, 43.44%, and 60.49%. The main drivers of CSD in the karst forest of Maolan were litter carbon input, total nitrogen, total phosphorus, and total SOC, and were litter carbon input at Yuntai Mountain and litter carbon input and neutral phosphatase at Dashahe. The results indicate that the core driver of CSD in the karst forest is litter carbon input, and this can be adjusted in the future to regulate the carbon sequestration capacity of SOC.

**Keywords:** karst forests; soil organic carbon; driving factors; carbon sequestration potential



**Citation:** Zhang, L.; Wang, Y.; Chen, J.; Feng, L.; Li, F.; Yu, L. Characteristics and Drivers of Soil Organic Carbon Saturation Deficit in Karst Forests of China. *Diversity* **2022**, *14*, 62. <https://doi.org/10.3390/d14020062>

Academic Editors: Michael Wink, Mladen Kućinić and Vlatka Mičetić Stanković

Received: 23 December 2021

Accepted: 14 January 2022

Published: 18 January 2022

**Publisher's Note:** MDPI stays neutral with regard to jurisdictional claims in published maps and institutional affiliations.



**Copyright:** © 2022 by the authors. Licensee MDPI, Basel, Switzerland. This article is an open access article distributed under the terms and conditions of the Creative Commons Attribution (CC BY) license (<https://creativecommons.org/licenses/by/4.0/>).

## 1. Introduction

Soils are considered the largest terrestrial pool of global carbon. Soil organic carbon (SOC) pool is an important and variable carbon reservoir in terrestrial ecosystems and a potential sink of greenhouse gases that can exhibit significant spatial variation [1,2]. The forest SOC pool is an important component of the forest ecosystem; 73% of global soil carbon is stored in forest soils. Therefore, it plays an irreplaceable role in maintaining the global climate system, regulating the global carbon balance, and slowing the rise of atmospheric greenhouse gas concentrations [3,4]. Small changes in this carbon pool, especially in the mineral particle organic carbon (<53 μm), will affect the global carbon balance and lead to global climate change [5].

Numerous studies have found that SOC eventually reaches equilibrium as exogenous carbon inputs continue to increase [6–8], i.e., soil carbon saturation [9]. Stewart et al. [10] and Feng et al. [11] estimated the maximum saturation of SOC in grassland, agricultural land, and forest by constructing a model of the maximum saturation capacity of SOC, thereby providing a foundation for subsequent studies on the carbon sequestration potential of SOC and the relevant influencing factors. In recent years, research on SOC in forest ecosystems has focused on the sequestration of SOC, decomposition of litter, and the influence of environmental factors on SOC at large spatial scales [12,13]. Zhou et al. [14]

found that soil carbon content in China's forest ecosystems accounted for 3/4 of the total forest ecosystem; Huang et al. [15] found that SOC content increased with the gradual recovery of vegetation, and soil carbon sequestration capacity was enhanced through the study of different vegetation restoration processes in Maolan. Zhang et al. [16] and Lal et al. [17] found that changes in soil carbon flux were mainly influenced by the interaction of vegetation, climate, and soil properties. Soil organic carbon saturation deficit (CSD) is equal to the maximum saturated capacity of SOC minus the current SOC [10], which is an important index directly reflecting soil carbon sequestration potential. Di et al. [18] found that in agricultural soils, increased application of organic fertilizers significantly reduced CSD over time, resulting in less space for future carbon sequestration, and carbon input was the main influence factor on CSD. At present, there have been few studies on the characteristics and drivers of saturation deficit in forest soils.

Karst forests are forest ecosystems that are distributed on landscapes with limestone, dolomite, and carbonate as the main bedrock. Plants in karst forests are constrained by soil topography [19,20]; as a unique ecosystem, the topography, hydrothermal conditions, and soil development conditions differ from those of non-karst areas [21–24]. Based on this complexity and specificity, the study of CSD in karst forest ecosystems is highly relevant. The key questions addressed in this study were: (1) What are the levels of CSD at different successional stages in karst forests, and how does this affect the future carbon sequestration potential? (2) What are the main drivers of CSD in karst forests, and how can they be regulated?

## 2. Materials and Methods

### 2.1. Overview of the Study Areas

The study areas were located in Maolan National Nature Reserve, Shibing Yuntai Mountain Nature Reserve, Daozhen Dashah Nature Reserve, Nayong Gongtong Nature Reserve, Pogang Karst Vegetation Nature Reserve, Kuankuoshui Nature Reserve, Puding Huoyan Mountain Nature Reserve, Jiangkou Huanggu Mountain Nature Reserve, Kaiyang Zijiang Geosuture, and Wangmo Bijia Mountain, all in Guizhou Province, China (Figure 1). These study areas are typical karst forests that present climax communities because they are long-established forests that experience low levels of disturbance, and thus they can be used to model the maximum saturation capacity of SOC in karst forests. Among these karst forests, three areas with rich successional stages were selected from south to north, namely, Maolan National Nature Reserve, Shibing Yuntai Mountain Nature Reserve, and Daozhen Dashah Nature Reserve, to explore CSD and the driving factors at different successional stages. The Maolan National Nature Reserve has a total area of 213 km<sup>2</sup> with a maximum elevation of 1079 m, a minimum elevation of 430 m, and an average elevation of 700 m. It has a central subtropical southern monsoon climate with an average annual temperature of 18.3 °C, annual precipitation of 1321 mm, and an annual sunshine duration of 1271 h. Most parts of the reserve are central subtropical primary karst forests, with mixed evergreen, deciduous broad-leaved tree species. There are different degrees of successional communities, with 1203 species of vascular plants in 154 families and 514 genera [15]. The Yuntai Mountain Nature Reserve has a total area of 47 km<sup>2</sup> with a maximum elevation of 1869 m, a minimum elevation of 486 m, and an average elevation of 526 m. It has a humid subtropical monsoon climate with an average annual temperature of 16.4 °C, annual precipitation of 1130 mm, and an annual sunshine duration of 1197 h. The reserve has the typical karst topography of southern China; the area is also a World Heritage Site with vegetation growing on dolomite rocks and a native and relatively stable karst forest [25]. The Dashah Nature Reserve has a total area of 270 km<sup>2</sup> with a maximum elevation of 1940 m, a minimum elevation of 564 m, and an average elevation of 1252 m. It has a humid monsoon climate with an average annual temperature of 12.1 °C, annual precipitation of 1194 mm, and an annual sunshine duration of 1134 h. The reserve is located in a karst landscape on soluble carbonate rock formations and is extremely rich in biological resources. There are 3594 species of plants in 1082 genera of 296 families and 208 species in 95 genera

of 47 families of macrofungi, making it one of the most valuable gene pools of biological species in the central subtropics of China [26].

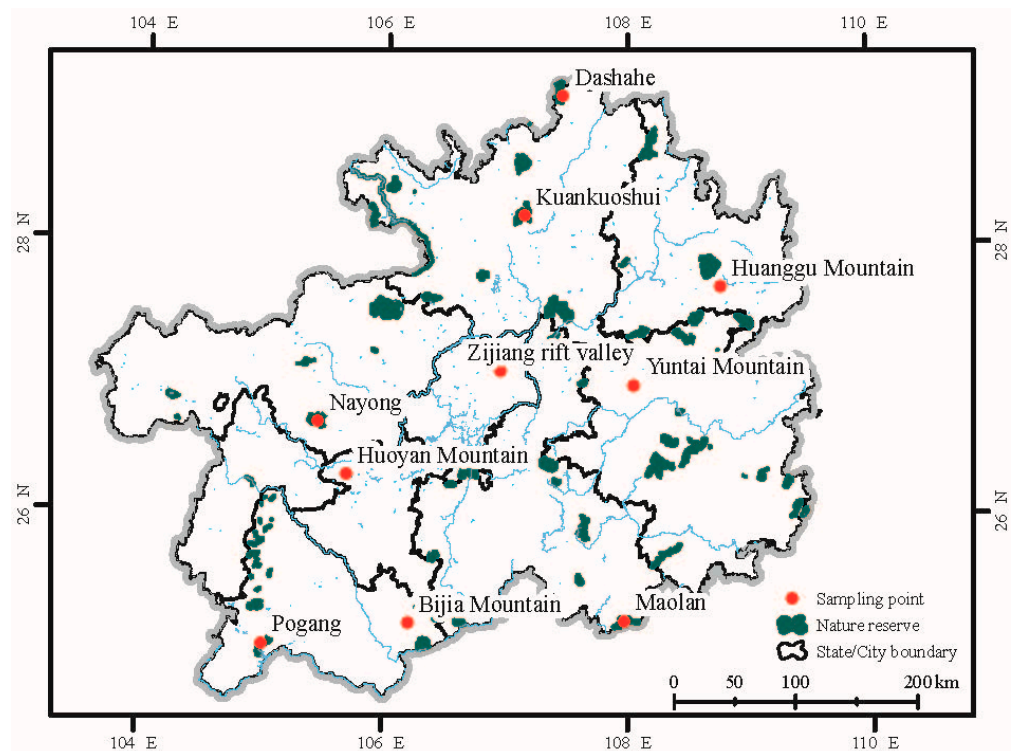


**Figure 1.** Distribution map of sample points.

## 2.2. Research Methodology

### 2.2.1. Sample Site Selection and Vegetation Survey

A total of 57 sample plots were established within seven typical karst forest climax communities, and three study areas in each of four different successional stages were selected from south to north, with three sample plots in each community. The sample plots were 2 m × 5 m for the herb stage, 4 m × 10 m for the shrub stage, 20 m × 20 m for the arbor stage, and 20 m × 20 m for the climax stage. Ten small sample squares were chosen in each sample plot for vegetation surveys. The surveys followed conventional community survey methods [27], where tree plant species, the number of plants, shrub and herb species, and habitat factors including elevation, height, slope degree, slope direction, and soil type were recorded in the sample plots. The information is shown in Tables 1 and 2.

**Table 1.** The basic information of the environmental background of different sample point.

Area	Succession Stage	Coordinates	Elevation (m)	Precipitation (mm)	Annual Mean Temperature (°C)	Aspect	Dominant Species	Soil Bedrock	Soil Type	Sample Size (m <sup>2</sup> )
Maolan	Herb stage	108.03 25.26	840	1590.70	19.75	NW	<i>Pteridium revolutum</i> , <i>Imperata cylindrical var. major</i> , <i>Pogonatherum crinitum</i> , <i>Trisetum bifidum</i>	Dolomite limestone	Clay, black limestone soil	2 × 5
	Shrub stage	107.94 25.30	820	1590.70	19.75	SW	<i>Pyracantha fortuneana</i> , <i>Nandina domestica</i> , <i>Lindera communis</i> , <i>Myrsine semiserrata</i> , <i>Clausena dunniana</i> , <i>Ulmus parvifolia</i>	Dolomite limestone	Clay, black limestone soil	4 × 10
	Arbor stage	107.95 25.29	840	1590.70	19.75	SW	<i>Swida wilsoniana</i> , <i>Machilus chienkweiensis</i> , <i>Lindera communis</i> , <i>Cladrastis platycarpa</i> , <i>Choerospondias axillaris</i>	Dolomite limestone	Clay, black limestone soil	20 × 20
	Climax stage	107.99 25.19	850	1590.70	19.75	SW	<i>Swida wilsoniana</i> , <i>Pittosporum brevicalyx</i> , <i>Cyclobalanopsis multiervis</i> , <i>Acerwangchii</i> , <i>Carpinus pubescens</i> , <i>Phoebe crassipedicella</i>	Dolomite limestone	Clay, black limestone soil	20 × 20
Yuntai Mountain	Herb stage	108.12 27.18	873	1083.80	17.29	SW	<i>Awn</i> , <i>Ophiopogon japonicus</i> , <i>Ficus tikoua</i> Bur., <i>Athyrium dissitifolium</i>	Carbonate rock	Clay, black limestone soil	2 × 5
	Shrub stage	108.16 27.13	865	1083.80	17.29	NW	<i>Bridelia tomentosa</i> , <i>Neillia sinensis</i> Oliv., <i>Viburnum dilatatum</i> Thunb., <i>Nothopanax davidii</i> Franch.Harms	Carbonate rock	Loam, black limestone soil	4 × 10
	Arbor stage	108.10 27.10	841	1083.80	17.29	SW	<i>Lindera communis</i> Hemsl., <i>Pistacia chinensis</i> Bunge, <i>Quercus acutissima</i> Carr., <i>Platycarya strobilacea</i>	Carbonate rock	Loam, black limestone soil	20 × 20
	Climax stage	108.11 27.12	875	1083.80	17.29	NW	<i>Cupressus funebris</i> , <i>Quercus dolicholepis</i> , <i>Platycarya strobilacea</i> , <i>Carpinus pubescens</i> , <i>Quercus phillyraeoides</i>	Carbonate rock	Loam, black limestone soil	20 × 20

Table 1. Cont.

Area	Succession Stage	Coordinates	Elevation (m)	Precipitation (mm)	Annual Mean Temperature (°C)	Aspect	Dominant Species	Soil Bedrock	Soil Type	Sample Size (m <sup>2</sup> )
Dashahae	Herb stage	107.58 29.15	1371	1372.20	16.81	NE	<i>Imperata cylindrica</i> , <i>Carex capilliformis</i> , <i>R. setchuenensis</i>	Carbonate rock	Clay, black limestone soil	2 × 5
	Shrub stage	107.57 29.10	1416	1372.20	16.81	NE	<i>Pyracantha fortuneana</i> , <i>Viburnum dilatatum</i> Thunb., <i>R. setchuenensis</i> , <i>Wild persimmon</i>	Carbonate rock	Clay, black limestone soil	4 × 10
	Arbor stage	108.01 29.12	1389	1372.20	16.81	NE	<i>Litsea elongata</i> Benth., <i>Machilus versicolora</i> , <i>Carpinus pubescens</i> Burk., <i>Fagus longipetiolata</i>	Carbonate rock	Loam, black limestone soil	20 × 20
	Climax stage	107.58 29.17	1304	1372.20	16.81	N	<i>Machilus pingii</i> , <i>Tetracentron sinense</i> , <i>Dipentodon sinicus</i> , <i>Davidia involucrata</i> , <i>Emmenopterys henryi</i>	Carbonate rock	Loam, black limestone soil	20 × 20
Nayong	Climax stage	105.44 26.68	1861	1226.00	14.75	NW	<i>Davidia involucrata</i> , <i>Decaisnea insignis</i> , <i>Dipentodon sinicus</i> , <i>Cyclobalanopsis argyrotricha</i>	Carbonate rock	Loam, black limestone soil	20 × 20
Pogang	Climax stage	105.09 25.11	1280	1501.70	17.10	N	<i>Eucalyptus robusta</i> , <i>Platycarya strobilacea</i> , <i>Itoa orientalis</i> Hemsl	Dolomite limestone	Loam, black limestone soil	20 × 20
Kuankuoshui	Climax stage	107.06 28.18	1450	1029.40	15.91	SW	<i>Fagus longipetiolata</i> , <i>Emmenopterys henryi</i> , <i>Tulip poplar</i>	Carbonate rock	Loam, black limestone soil	20 × 20
Huoyan mountain	Climax stage	105.79 26.47	1680	1163.10	15.98	W	<i>Rhododendron stamineum</i> , <i>Birch</i> , <i>Oak</i>	Carbonate rock	Loam, black limestone soil	20 × 20
Huanggu mountain	Climax stage	108.78 27.54	1020	1542.00	17.56	N	<i>Fagus longipetiolata</i> , <i>Buxus sinica</i> , <i>Davidia involucrata</i> , <i>Hemlock</i>	Carbonate rock	Loam, black limestone soil	20 × 20
Zijiang rift valley	Climax stage	107.04 26.90	720	1169.00	14.13	SW	<i>Betula luminifera</i> , <i>Cinnamomum camphora</i> , <i>Pistacia chinensis</i> , <i>Liquidambar formosana</i>	Carbonate rock	Loam, black limestone soil	20 × 20
Bijia mountain	Climax stage	106.14 25.12	1083	1062.70	20.53	NW	<i>Cyclobalanopsis oak</i> , <i>Carpinus pubescens</i> , <i>Celtis sinensis</i> , <i>Ormosia saxatilis</i>	Carbonate rock	Loam, black limestone soil	20 × 20

**Table 2.** The basic information of soil physical and chemical properties in different succession stages.

Area	Succession Stage	pH	BD (g cm <sup>-3</sup> )	SOC (g kg <sup>-1</sup> )	TN (g kg <sup>-1</sup> )	TP (g kg <sup>-1</sup> )	Lci (g C m <sup>-2</sup> )	Ca (g kg <sup>-1</sup> )	Ur (mg g <sup>-1</sup> 24 h <sup>-1</sup> )	Npa (mg g <sup>-1</sup> 24 h <sup>-1</sup> )	Sa (mg g <sup>-1</sup> 24 h <sup>-1</sup> )
Maolan	Herb stage	7.34 ± 0.08a	1.31 ± 0.02a	28.34 ± 2.80d	1.57 ± 0.03d	0.36 ± 0.01d	12.27 ± 1.08d	1.38 ± 0.05c	0.09 ± 0.01c	0.65 ± 0.08b	7.08 ± 0.23b
	Shrub stage	7.63 ± 0.07a	1.25 ± 0.01a	65.30 ± 4.36c	6.75 ± 0.43c	1.01 ± 0.10b	33.57 ± 2.44c	3.19 ± 0.48b	0.89 ± 0.48b	2.62 ± 0.15a	7.36 ± 0.14b
	Arbor stage	7.23 ± 0.06a	1.20 ± 0.01a	85.22 ± 3.69b	7.55 ± 0.11b	0.77 ± 0.02c	81.76 ± 2.23b	4.83 ± 0.14a	1.05 ± 0.11b	2.16 ± 0.34a	8.22 ± 0.22b
	Climax stage	7.14 ± 0.27a	1.02 ± 0.03b	94.13 ± 3.51a	8.42 ± 1.10aa	1.21 ± 0.20a	141.03 ± 2.53a	4.83 ± 1.02a	1.62 ± 0.45a	2.79 ± 0.33a	12.77 ± 0.73a
Yuntai Mountain	Herb stage	8.12 ± 0.05a	1.43 ± 0.06a	22.52 ± 1.23c	1.88 ± 0.08d	0.43 ± 0.01a	23.33 ± 1.34c	2.29 ± 0.09d	0.35 ± 0.04c	0.62 ± 0.04b	0.75 ± 0.08c
	Shrub stage	7.94 ± 0.02a	1.28 ± 0.03b	41.46 ± 2.05b	3.67 ± 0.22c	0.64 ± 0.01a	40.39 ± 2.19c	4.49 ± 0.19c	3.18 ± 0.09b	2.20 ± 0.07a	1.36 ± 0.12c
	Arbor stage	7.97 ± 0.04a	1.19 ± 0.04c	58.84 ± 3.16b	5.43 ± 0.25b	0.57 ± 0.02a	137.09 ± 6.90b	6.63 ± 0.14a	4.18 ± 0.30a	2.26 ± 0.09a	9.86 ± 1.99b
	Climax stage	7.93 ± 0.06a	1.17 ± 0.02c	82.13 ± 2.48a	6.75 ± 0.79a	0.54 ± 0.03a	181.11 ± 6.72a	5.09 ± 0.74b	4.25 ± 0.76a	2.08 ± 0.24a	12.83 ± 0.82a
Dashahe	Herb stage	7.49 ± 0.22a	1.30 ± 0.02a	18.35 ± 2.13d	1.84 ± 0.03d	0.51 ± 0.04a	21.27 ± 8.71c	2.26 ± 0.38b	0.22 ± 0.04c	0.55 ± 0.08c	5.87 ± 2.12b
	Shrub stage	6.55 ± 0.04a	1.18 ± 0.03b	29.23 ± 3.05c	2.33 ± 0.17c	0.37 ± 0.01b	29.25 ± 2.34c	1.85 ± 0.13c	0.35 ± 0.03c	0.69 ± 0.03c	4.67 ± 1.51b
	Arbor stage	6.60 ± 0.10a	1.22 ± 0.02b	49.93 ± 3.52b	3.77 ± 0.29b	0.39 ± 0.01b	98.86 ± 7.55b	2.83 ± 0.25b	0.74 ± 0.10b	1.89 ± 0.14a	10.60 ± 1.91a
	Climax stage	7.74 ± 0.09a	1.12 ± 0.01c	78.75 ± 2.48a	5.53 ± 0.67a	0.69 ± 0.03a	204.71 ± 12.24a	3.20 ± 0.31a	2.28 ± 0.75a	1.12 ± 0.14b	11.11 ± 1.74a

Note: BD is soil bulk density, SOC is soil total organic carbon, TN is total nitrogen, TP is total phosphorus, Lci is litter carbon input, Ca is exchangeable calcium, Ur is soil urease, Npa is neutral phosphatase, Sa is soil sucrase. Different lowercase letters indicate a significant difference ( $p < 0.05$ ) among different succession stages for soil property. Contents are reported as mean ± SE.

### 2.2.2. Soil Sample Collection and Processing

Surface soil samples were collected in each sample plot along two diagonal lines within the square plot using the “S” type five-point mixed sampling method. Three mixed samples were collected from each sample plot for a total of 171 soil samples from 57 sample plots, while 3 soil samples were collected by 100 cm<sup>3</sup> foil sampler from each sample plot for a total of 171 and dried for the determination of soil bulk density. Sampling was carried out by removing litter from the surface and removing gravel and roots that were visible to the naked eye after sampling and mixing. One sample from each of the Maolan, Yuntai Mountain, and Dashahe Nature Reserves was taken back to the laboratory in a sealed plastic bag, air-dried, and finely ground through a 0.25 mm sieve; the other sample was taken back to the laboratory in a low-temperature sampling box and placed in an ultra-low temperature refrigerator at −70 °C for microbiological determination. Soil samples from the seven climax communities were brought back to the laboratory in sealed plastic bags, air-dried, finely ground, and passed through a 0.25 mm sieve.

### 2.2.3. Litter Sample Collection and Processing

Nylon mesh was used to construct a square sampling frame with an area of 1.0 m<sup>2</sup>. We randomly selected three small subplots in each plot at the shrub, arbor, and climax stages to sample the litter. The square sampling frame was placed horizontally during sampling. The litter in the square sampling frame was collected every six months. For the herb stage, three small 1.0 m<sup>2</sup> subplots were randomly selected in each plot, and the aboveground plant parts were harvested as the litter. A total of 36 samples were collected. All samples were brought back to the laboratory in sealed plastic bags, dried in an oven at 60 °C to a constant weight, and partly ground and passed through a 0.25 mm sieve to determine the carbon content of the litter.

### 2.2.4. SOC Fraction

The wet sieving method of Six et al. [28] was used to determine the SOC fraction. The procedure was as follows: 30 g of air-dried soil sample was passed through a 2 mm sieve and then placed on the top sieve of a microaggregate separator set (top 250 µm sieve, bottom 53 µm sieve). Then, 15 glass beads were added, and after the separator was shaken for 30 min, the >250 µm agglomerates remained on the top sieve; the microaggregate fraction was retained on the 53–250 µm sieve, and soil particles that passed through the 53 µm sieve comprised the fine particle fraction. Then, 25 mL of 0.25 mol/L CaCl<sub>2</sub> solution was added to the bucket of the <53 µm sieve, and the mixture was centrifuged at 1730 × *g* for 15 min to separate the fine particle fraction. All fractions were transferred to aluminum boxes, steamed using a water bath, and then dried in an oven at 60 °C for 12 h. After drying, the fractions were finely ground and sieved through a 0.25 mm sieve and used to determine the SOC content of each fraction.

### 2.2.5. Methods for Determination of Soil Sample Indicators

Soil physical and chemical properties were determined using the methods described in *Soil Agrochemical Analysis* by Bao Shidan [29]. The specific methods for each soil property were as follows. Soil pH: the potentiometric method with a soil–liquid ratio of 1:2.5; soil bulk density: cutting ring weighing method; SOC: the oil bath heating potassium dichromate oxidative capacity method; soil total nitrogen: the Kjeldahl distillation method; soil total phosphorus: the molybdenum antimony anti-colorimetric method; soil total potassium: the sodium hydroxide fusion-flame photometric method; exchangeable calcium: the ammonium acetate exchange-atomic absorption spectrophotometric method. Soil enzymes were determined by the methods listed in *Soil enzymes and their research methods* by Song-Ying Guan [30]. Soil urease was determined by the phenol-sodium hypochlorite colorimetric method; soil sucrase was determined using the 3,5-dinitrosalicylic acid colorimetric method; soil phosphatase was determined by the sodium phosphate colorimetric method.

### 2.3. Data Processing and Analysis

The SOC maximum saturation capacity model was constructed using the boundary line method of Feng [11] implemented by setting a boundary limit value (top 10%), equivalent to dividing the <53  $\mu\text{m}$  fine particle fraction carbon of the 10 karst forest climax communities into 9 groups and extracting the top 10% of the fine particle fraction. Using the corresponding mass proportions from each group of data, the data were used for linear regression, and the intercept was forced through the zero point to construct a model of the maximum saturation capacity of SOC in karst forests. The maximum saturation capacity of SOC in the three regions was estimated using the regression model. The CSD at each successional stage was defined as the difference between the maximum saturation capacity of SOC and the current SOC.

The data obtained were processed using Excel 2007 software, and statistical analysis was performed using SPSS 19.0 software and Duncan's new complex polar difference method.  $p < 0.05$  was considered as significant. Statistical analysis and driver screening were performed using R language software [31].

## 3. Results

### 3.1. Characteristics of Changes in SOC Content

The carbon fractions and SOC contents in different successional stages all showed significant differences (Table 3). The carbon fraction and SOC content of karst forest soil at different successional stages followed the pattern of climax stage > arbor stage > shrub stage > herb stage, and the SOC contents of the soils in the climax stages of Maolan, Yuntai Mountain, and Dashahe were 94.13, 82.13, and 78.75  $\text{g C kg}^{-1}$  soil, values that were 3.32, 1.44, and 1.10 times, 3.65, 1.98, and 1.40 times, and 4.29, 2.69, and 1.58 times higher than those in the herb, shrub, and arbor stages, respectively. The SOC content of each successional stage in different karst forests followed the order Maolan > Yuntai Mountain > Dashahe. Among the 10 climax communities, the <53  $\mu\text{m}$  carbon fraction and the SOC content were the highest in Nayong, with 23.56 and 147.11  $\text{g C kg}^{-1}$  soil, respectively, and were lowest in Zijiang Geosuture at 8.30 and 42.05  $\text{g C kg}^{-1}$  soil, respectively. The proportion of <53  $\mu\text{m}$  organic carbon in SOC did not show significant differences among the 10 climax communities, with a mean value of 19.44%.

**Table 3.** Contents change of soil total organic carbon and fraction carbon.

Area	Succession Stage	>250 $\mu\text{m}$ Fraction C Content ( $\text{g C kg}^{-1}$ Soil)	53–250 $\mu\text{m}$ Fraction C Content ( $\text{g C kg}^{-1}$ Soil)	<53 $\mu\text{m}$ Fraction C Content ( $\text{g C kg}^{-1}$ Soil)	Soil Organic C Content ( $\text{g C kg}^{-1}$ Soil)	Proportion of <53 $\mu\text{m}$ C to Total Organic C ( $\text{g Fraction } 100\text{g}^{-1}$ Soil)
Maolan	Herb stage	17.33 $\pm$ 0.62d	7.50 $\pm$ 0.46d	3.51 $\pm$ 0.38d	28.34 $\pm$ 2.80d	12.39 $\pm$ 0.55c
	Shrub stage	31.91 $\pm$ 1.50c	22.77 $\pm$ 1.19c	10.62 $\pm$ 0.68c	65.30 $\pm$ 4.36c	16.26 $\pm$ 0.43b
	Arbor stage	39.49 $\pm$ 2.46b	30.35 $\pm$ 2.55b	15.38 $\pm$ 1.29b	85.22 $\pm$ 3.69b	18.05 $\pm$ 0.62a
	Climax stage	43.77 $\pm$ 2.35aB	33.19 $\pm$ 2.33aB	17.17 $\pm$ 0.73aB	94.13 $\pm$ 3.51aB	18.24 $\pm$ 1.03aA
Yuntai Mountain	Herb stage	17.32 $\pm$ 1.12c	3.31 $\pm$ 0.29d	1.89 $\pm$ 0.19c	22.52 $\pm$ 0.84d	8.39 $\pm$ 0.21b
	Shrub stage	20.70 $\pm$ 1.23c	16.70 $\pm$ 1.61c	4.06 $\pm$ 0.21c	41.46 $\pm$ 1.75c	9.79 $\pm$ 0.32b
	Arbor stage	27.58 $\pm$ 2.67b	20.58 $\pm$ 3.31b	10.68 $\pm$ 0.98b	58.84 $\pm$ 4.61b	18.15 $\pm$ 0.65a
	Climax stage	38.06 $\pm$ 1.48aB	27.97 $\pm$ 1.70aBC	16.10 $\pm$ 2.48aB	82.13 $\pm$ 2.08aC	19.60 $\pm$ 0.24aA
Dashahe	Herb stage	14.69 $\pm$ 1.10c	2.20 $\pm$ 0.21d	1.46 $\pm$ 0.19c	18.35 $\pm$ 0.97d	7.96 $\pm$ 0.13c
	Shrub stage	17.46 $\pm$ 0.82c	9.58 $\pm$ 0.96c	2.19 $\pm$ 0.24c	29.23 $\pm$ 0.84c	7.49 $\pm$ 0.28c
	Arbor stage	28.93 $\pm$ 2.63b	15.25 $\pm$ 1.74b	5.75 $\pm$ 0.52b	49.93 $\pm$ 3.21b	11.52 $\pm$ 0.44b
	Climax stage	39.01 $\pm$ 2.01aB	24.22 $\pm$ 2.13aC	15.52 $\pm$ 0.81aB	78.75 $\pm$ 2.45aCD	19.71 $\pm$ 0.36aA
Nayong	Climax stage	69.21 $\pm$ 3.42A	54.34 $\pm$ 4.51A	23.56 $\pm$ 3.87A	147.11 $\pm$ 6.55A	18.42 $\pm$ 0.52A
Pogang	Climax stage	41.69 $\pm$ 4.74B	24.65 $\pm$ 2.58C	15.44 $\pm$ 1.43B	81.78 $\pm$ 8.89C	18.88 $\pm$ 0.34A
Kuankuoshui	Climax stage	29.06 $\pm$ 1.99C	18.99 $\pm$ 1.23D	11.45 $\pm$ 0.28C	59.50 $\pm$ 4.79DE	19.24 $\pm$ 1.17A
Huoyan mountain	Climax stage	28.22 $\pm$ 1.53C	12.18 $\pm$ 0.93E	9.03 $\pm$ 1.73D	49.43 $\pm$ 0.63E	21.09 $\pm$ 0.70A
Huanggu mountain	Climax stage	39.65 $\pm$ 1.56B	20.52 $\pm$ 0.76D	15.62 $\pm$ 1.77B	75.79 $\pm$ 1.39CD	20.61 $\pm$ 2.26A
Zijiang rift valley	Climax stage	17.95 $\pm$ 0.69D	15.80 $\pm$ 0.99DE	8.30 $\pm$ 0.78D	42.05 $\pm$ 1.85F	19.74 $\pm$ 1.76A
Bijia mountain	Climax stage	32.20 $\pm$ 2.15C	20.95 $\pm$ 1.64D	12.26 $\pm$ 1.49C	65.41 $\pm$ 6.03D	18.82 $\pm$ 0.25A

Note: Different lowercase letters indicate a significant difference ( $p < 0.05$ ) among different succession stages, different capital letters indicate a significant difference ( $p < 0.05$ ) among different climax stages for each fraction, C content and proportion are reported as mean  $\pm$  SE.



### 3.2. CSD Characteristics

The maximum saturation capacity of SOC in karst forests was modelled as  $y = 0.66x$  ( $R^2 = 0.78$ ) (Figure 2), and the maximum saturation values of SOC in Maolan, Yuntai Mountain, and Dashahe were 20.70%, 18.88%, and 14.55%, respectively, according to the model. The CSD in karst forests showed significant differences at different successional stages (Figure 3). The CSD in the herb stage was the highest in Maolan, Yuntai Mountain, and Dashahe at 83.04%, 89.99%, and 89.97%, respectively, followed by the shrub stage at 48.69%, 78.50%, and 84.95%, and the lowest in the arbor stage at 25.69%, 43.44%, and 60.49%. The CSD values in the herb stage were 1.71, 1.15, and 1.06 and 3.23, 2.07, and 1.49 times higher than those in the shrub and arbor stages, respectively. The CSD in karst forests showed an overall increasing trend from south to north.

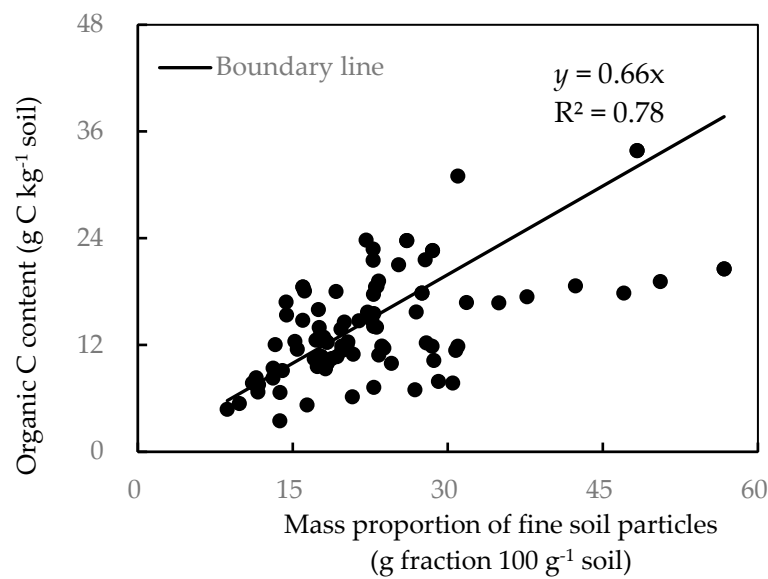


**Figure 2.** Boundary line analysis of organic C content ( $\text{g C kg}^{-1}$  soil) of  $<53 \mu\text{m}$  particles with their mass proportions ( $\text{g fraction } 100 \text{ g}^{-1}$  soil) in all bulk soils.

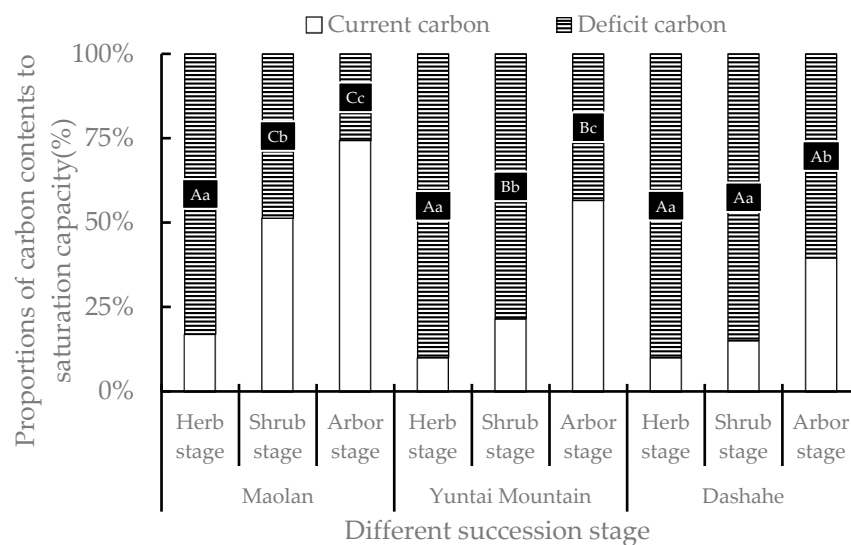


**Figure 3.** Saturated deficit of soil organic carbon at different succession stages in different regions (Note: Different lowercase letters indicate a significant difference ( $p < 0.05$ ) among different succession stages, different capital letters indicate a significant difference ( $p < 0.05$ ) among different regions).

### 3.3. Analysis of the Main Drivers of CSD

The main drivers of CSD differed significantly between karst forests (Table 4). In Maolan, the multiple stepwise regression model showed a significant relationship between CSD and litter carbon input, total nitrogen, total phosphorus, and total SOC, with an  $R^2$  of 0.96 and a significant model fit ( $p < 0.01$ ). In Yuntai Mountain, the regression model showed that the CSD was linearly related to the amount of litter carbon input ( $R^2 = 0.90$ ;  $p < 0.05$ ). In Dashahe, the stepwise regression model showed a significant relationship between CSD and litter carbon input and neutral phosphatase (corrected  $R^2 = 0.91$ ;  $p < 0.05$ ). All three karst forests showed a significant regression between CSD and litter carbon input, and the larger the coefficient, the smaller the contribution to CSD. The trend of CSD was Maolan > Yuntai Mountain > Dashahe when equal amounts of litter were considered.

**Table 4.** Regression model between soil organic carbon saturation deficit (CSD) and major driving factors.

Different Regions	Regression Equation	Indicative Factor	p Value	Correction $R^2$
Maolan	$y = -0.45x_1 - 6.22x_2 + 43.85x_3 - 0.42x_4 + 94.38$	y: CSD x <sub>1</sub> : Lci x <sub>2</sub> : TN x <sub>3</sub> : TP x <sub>4</sub> : SOC	0.001	0.96
Yuntai Mountain	$y = -0.40x_1 + 97.15$	y: CSD x <sub>1</sub> : Lci	0.000	0.90
Dashahe	$y = -0.16x_1 - 11.49x_2 + 98.59$	y: CSD x <sub>1</sub> : Lci x <sub>2</sub> : Npa	0.001	0.91

Note: CSD is soil organic carbon saturation deficit, Lci is litter carbon input, TN is total nitrogen, TP is total phosphorus, SOC is soil total organic carbon, Npa is neutral phosphatase.

## 4. Discussion

### 4.1. Characteristics of the Changes in SOC Content

The results of this study demonstrated that the carbon fraction and SOC content increased as succession progressed, consistent with the results of other studies [32,33] and indicating that the climax stage is the main carbon sink of karst forest ecosystems and that it has a high carbon sequestration capacity. The main reason for this is that the litter carbon input increased significantly as succession progressed (Table 2), with 12.27 g/m<sup>2</sup>, 23.33 g/m<sup>2</sup>, and 21.27 g/m<sup>2</sup> in the herb stage of Maolan, Yuntai Mountain, and Dashahe, respectively, reaching 141.03 g/m<sup>2</sup>, 181.11 g/m<sup>2</sup>, and 204.71 g/m<sup>2</sup> in the climax stage, values that were 11.49 and 7.76 times higher than those in the herb stage. The amount of litter carbon input is the main source of forest soil carbon and directly affects the SOC balance [15,34,35]. Meanwhile, a large number of studies have found that increased carbon input may have a negative excitation effect on soil original organic carbon and inhibit its native soil organic carbon [19,36,37]. The root system is also a source of soil carbon input, and the dominant tree species in both the arbor and climax stages were mixed with evergreen, deciduous broad-leaved trees (Table 1) with well-developed root systems and greater carbon input to the soil. In contrast, the dominant species in the herb and shrub stages were herbs or shrubs (Table 1) with less-developed root systems and less carbon input to the soil. The soil microorganisms play a crucial role in the SOC sequestration process, regulating the SOC balance in both directions [38,39]. The successional sequence from the herb stage to the climax stage can improve the soil agglomeration structure by increasing microbial biomass, especially fungal mycelia; this increases soil organic cementation that in turn increases the physical conservation of SOC [36,40]. The structure and activity of soil microbial communities differ at various successional stages, and fungal cell residues, especially cell wall components, are more difficult to decompose than bacteria. Thus it

is possible that a higher proportion of fungi in the climax stage increases the stability of SOC [6,41].

Many studies have suggested that climatic factors, especially temperature and precipitation, are the most important determinants of SOC distribution at large scales [18,37,42]. The positive relationship between temperature and precipitation and SOC in forests has been highlighted in global and more regional studies [43,44]. In our study, there were significant differences in SOC content among the karst forests with different temperatures and precipitation. Maolan had the highest temperature and precipitation (19.75 °C, 1590.70 mm) (Table 2), and SOC content was also the highest. On the contrary, Dashahe had the lowest temperature (16.81 °C) and average precipitation (1372.20 mm) (Table 2), and SOC content was the lowest. This is consistent with the results from studies on a global scale and numerous regional scales [33,45]. Temperature and precipitation increase could significantly enhance the bio-productivity and accelerate the decomposition rate of litter, thus increasing the input of SOC. When the amount of exogenous carbon input is greater than the amount of SOC mineralization, it is beneficial to the accumulation of SOC [45,46].

#### 4.2. Characteristics of the Changes in CSD

CSD is an indicator of the level of future carbon sequestration potential of SOC or the amount of space available for sequestration [47]. The greater the CSD, the greater the potential for future sequestration of SOC. In this study, CSD was highest in the herb stages of Maolan, Yuntai Mountain, and Dashahe at 83.04%, 89.99%, and 89.97%, respectively, followed by 48.69%, 78.50%, and 84.95% in the shrub stage and being lowest in the arbor stage at 25.69%, 43.44%, and 60.49% (Figure 3), indicating that as succession progressed, the CSD decreased. The future carbon sequestration potential gradually decreased, i.e., the herb stage had the most space for carbon sequestration, followed by the shrub and arbor stages. In the three karst forests, the CSD was not significantly different between the herb stages of Maolan, Yuntai Mountain, and Dashahe, while there was a trend of Dashahe > Yuntai Mountain > Maolan at the shrub and arbor stages. On the whole, the CSD showed a gradual increase from south to north, indicating that the future carbon sequestration potential of Dashahe is the largest, followed by Yuntai Mountain and Maolan. On a large spatial scale, Xu et al. [48] found that the CSD in the surface layer of the Daxinganling Forest was 2.20% and 78.80% in the deep layer, indicating that the deep layer had a greater potential for carbon sequestration. Zhang [49] found that the CSD in a protected forest in a desert zone was 27.58%. CSD varies from region to region and is related to the maximum saturation of SOC and the organic carbon content of existing soil mineral particles [9]. In this study, the CSD was related to the organic carbon content of the <53 µm fraction, and the closer the organic carbon content of the <53 µm fraction to the climax stage, the lower the CSD, and the opposite is true. In this study, as succession proceeded, the organic carbon content of the <53 µm fraction increased and was greatest in the karst forest at Maolan, lower at Yuntai Mountain, and least at Dashahe (Table 3). Therefore, regarding the future of karst forests, development should be conducted from north to south as far as possible, and priority should be given to grassland and shrub stages in order to achieve the maximum relative carbon sequestration capacity.

#### 4.3. Analysis of the Main Drivers of the CSD

CSD is influenced by multiple interacting factors and involves complex processes [50–53]. In this study, the main drivers of CSD in different karst forests were litter carbon input, total nitrogen, total phosphorus, and total SOC in Maolan, litter carbon input in Yuntai Mountain, and litter carbon input and neutral phosphatase in Dashahe. The results showed that the ecosystem structure of Maolan was the most complex among the different karst forests, and there was an overlap of environmental factors. Therefore, the CSD was influenced by multiple factors. Yuntai Mountain and Dashahe have relatively simple ecosystem structures, so there are few controlling factors. Litter carbon input is the main driving factor of CSD in karst forests, reflecting the important role of litter in maintaining soil carbon

balance in karst forests. As the main source of the soil carbon pool, litter decomposition and accumulation will affect the dynamic balance of SOC [54,55]. The amount of carbon input to litter is controlled by litter quality and external environmental conditions, and these two factors can be adjusted to control the litter carbon input [56,57]. Litter regulates CSD by affecting multiple factors such as soil microbial community structure and native soil organic carbon excitation. Phosphatase is one of the most active enzymes in soil. It is an important indicator enzyme for the characterization of soil biological activity, and it plays an important role in soil phosphorus cycling [58]. In this study, neutral phosphatase might affect carbon sequestration by changing soil fertility or might affect the amount of litter carbon input by changing the phosphorus absorption capacity of plants, thus affecting CSD. The results of this study were generally consistent with those of other researchers. Tian et al. [59] found that the factors affecting SOC stability at different elevation gradients were temperature, litter, and soil physicochemical properties. Liu et al. [60] found that the main controlling factors of SOC in Moso bamboo forests were soil porosity, capacitance, and soil enzyme activity. Guan et al. [45] found that the main influencing factors of SOC in northwestern forest ecosystems were standing age, temperature, humidity, elevation, and litter. In conclusion, although the main drivers of CSD in karst forests vary, the core driver is the amount of litter carbon input; therefore, this factor could be adjusted to regulate CSD in the future.

## 5. Conclusions

By constructing the maximum saturated capacity model of SOC in karst forests, we estimated the saturated deficit of SOC in different regions and succession stages and analyzed its main driving factors. The soil carbon fraction and SOC content in karst forests followed the pattern climax stage > arbor stage > shrub stage > herb stage, and the SOC content in different karst forests was Maolan > Yuntai Mountain > Dashahe. The CSD in the herb stages of Maolan, Yuntai Mountain, and Dashahe were the highest, and the future carbon sequestration potential of the herb stage was increased from south to north, with greater potential for exploitation. The core driver of CSD in forest ecosystems of the karst forests is the amount of litter carbon input, which can be adjusted to control CSD in karst forests.

**Author Contributions:** Conceptualization, L.Z. and L.Y.; methodology, J.C. and Y.W.; formal analysis, L.Z.; investigation, F.L. and L.F.; resources, L.Y.; writing—original draft preparation, L.Z.; writing—review and editing, L.Z.; supervision, L.Y.; funding acquisition, L.Y. All authors have read and agreed to the published version of the manuscript.

**Funding:** This research was funded by the Project of National Key Research and Development Program of China (grant number 2016YFC0502604); the Application Foundation Major Project of Guizhou Province of China (Qian Ke He JZ [2014] 2002); the Construction Program of Biology First-class Discipline in Guizhou of China (GNYL [2017]009); and the Project of Promoted Innovation of Colleges and Universities of Guizhou Province of China (Qian Jiao He Collaborative Innovation [2014]01).

**Institutional Review Board Statement:** No animal interventions were used in this research.

**Data Availability Statement:** All data are available on request.

**Acknowledgments:** We sincerely thank Meng Xu and his team for their help and support during the manuscript writing process.

**Conflicts of Interest:** The authors declare no conflict of interest.

## Abbreviations

SOC: Soil organic carbon; CSD: Carbon saturation deficit.

## References

- Panja, P. Deforestation, Carbon dioxide increase in the atmosphere and global warming: A modelling study. *Int. J. Model. Simul.* **2019**, *3*, 209–219. [\[CrossRef\]](#)
- Samaneh, T.; Shamsollah, A.; Mojtaba, Z. Digital mapping of soil organic carbon using ensemble learning model in Mollisols of Hyrcanian forests, northern Iran. *Geoderma Reg.* **2020**, *20*, e00256. [\[CrossRef\]](#)
- Mojtaba, Z.; Garosi, Y.; Reza, O.H.; Ayoubi, S.; Taghizadeh, M.R.; Scholten, T.; Xu, M. Improving the spatial prediction of soil organic carbon using environmental covariates selection: A comparison of a group of environmental covariates. *Catena* **2021**, *208*, 105727. [\[CrossRef\]](#)
- Zhu, J.X.; Hu, H.F.; Tao, S.L.; Chi, X.L.; Jiang, L.; Ji, C.J.; Zhu, J.L.; Tang, Z.Y.; Pan, Y.D.; Richard, A.B. Carbon stocks and changes of dead organic matter in China's forests. *Nat. Commun.* **2017**, *1*, 151. [\[CrossRef\]](#) [\[PubMed\]](#)
- Tao, Y.J.; Duan, M.S.; Deng, Z. Using an extended theory of planned behaviour to explain willingness towards voluntary carbon offsetting among Chinese consumers. *Ecol. Econ.* **2021**, *2*, 174–185. [\[CrossRef\]](#)
- Sayer, E.J.; Baxendale, C.; Birkett, A.J.; Bréchet, L.M.; Castro, B.; Deirdre, K.B.; Luis, L.S.; Chadtip, R. Altered litter inputs modify carbon and nitrogen storage in soil organic matter in a lowland tropical forest. *Biogeochemistry* **2020**, *1*, 23–34. [\[CrossRef\]](#)
- Zhuang, Y.; Zhu, J.; Shi, L.; Fu, Q.L.; Hu, H.Q.; Huang, Q.Y. Influence mechanisms of iron, aluminum and manganese oxides on the mineralization of organic matter in paddy soil. *J. Environ. Manag.* **2021**, *301*, 10–20. [\[CrossRef\]](#)
- Almeida, F.J.; Souza, I.F.; Hurtarte, C.C.; Teixeira, P.P.C.; Inagaki, T.M.; Silva, I.R.; Mueller, C.W. Forest litter constraints on the pathways controlling soil organic matter formation. *Soil Biol. Biochem.* **2021**, *4*, 142–153. [\[CrossRef\]](#)
- West, T.O.; Six, J. Considering the influence of sequestration duration and carbon saturation on estimates of soil carbon capacity. *Clim. Chang.* **2007**, *80*, 25–41. [\[CrossRef\]](#)
- Stewart, C.E.; Plante, A.F.; Paustian, K.P.; Conant, R.T.; Six, J. Soil carbon saturation: Linking concept and measurable carbon pools. *Soil Sci. Soc. Am. J.* **2008**, *72*, 379–392. [\[CrossRef\]](#)
- Feng, W.T.; Plante, A.F.; Six, J. Improving estimates of maximal organic carbon stabilization by fine soil particles. *Biogeochemistry* **2013**, *112*, 81–93. [\[CrossRef\]](#)
- Liu, G.H.; Fu, B.J.; Fang, J.Y. Carbon dynamics of Chinese forests and its contribution to global carbon balance. *Acta Ecol. Sin.* **2000**, *5*, 733–740.
- Sun, K.; Li, J.Q.; Yang, G.L.; Zhuo, M.; Hu, J. Effect of alterations in forest litter inputs on soil C and N storage distribution in pinus yunnanensis forest in central Yunnan Plateau. *Acta Ecol. Sin.* **2021**, *41*, 3100–3110. [\[CrossRef\]](#)
- Zhou, Y.R.; Yu, Z.L.; Zhao, S.D. Carbon storage and budget of major Chinese forest types. *Chin. J. Plant Ecol.* **2000**, *24*, 518–522.
- Huang, Z.S.; Yu, L.F.; Fu, Y.H.; Yang, R. Characteristics of carbon sequestration during natural restoration of Maolan karst forest ecosystems. *Chin. J. Plant Ecol.* **2015**, *39*, 554–564.
- Zhang, L.; Zhang, D.L.; Mao, Z.J. Characteristic mineralization of soil organic carbon in different successional series of broadleaved Korean pine forests in the temperate zone in China. *Acta Ecol. Sin.* **2017**, *37*, 6370–6378. [\[CrossRef\]](#)
- Lai, R.; Follett, R.F.; Stewart, B.A.; Kimble, J.M. Soil carbon sequestration to mitigate climate change and advance food security. *Soil Sci.* **2007**, *172*, 943–956. [\[CrossRef\]](#)
- Di, J.Y.; Xu, M.G.; Zhang, W.J.; Tong, X.G.; He, X.H.; Gao, H.J.; Liu, H.; Wang, B.R. Combinations of soil properties, carbon inputs and climate control the saturation deficit dynamics of stable soil carbon over 17-year fertilization. *Sci. Rep.* **2018**, *8*, 12653. [\[CrossRef\]](#)
- Yu, L.F. Research on Ecological Process of Natural Restoration of Degraded Karst Forest. Ph.D. Thesis, Nanjing Forestry University, Nanjing, China, 1998.
- Hamer, U.; Marschner, B. Priming effects in different soil types induced by fructose, alanine, oxalic acid and catechol additions. *Soil Biol. Biochem.* **2005**, *37*, 445–454. [\[CrossRef\]](#)
- Rietz, D.N.; Haynes, R.J. Effects of irrigation-induced salinity and sodicity on soil microbial activity. *Soil Biol. Biochem.* **2003**, *35*, 845–854. [\[CrossRef\]](#)
- Hu, N.; Li, H.; Tang, Z.; Li, Z.F.; Li, G.C.; Jiang, Y.; Hu, X.M.; Lou, Y.L. Community size, activity and C:N stoichiometry of soil microorganisms following reforestation in a Karst region. *Eur. J. Soil Biol.* **2016**, *73*, 77–83. [\[CrossRef\]](#)
- Liu, S.J.; Zhang, W.; Wang, K.L.; Pan, F.J.; Yang, S.; Shu, S.Y. Factors controlling accumulation of soil organic carbon along vegetation succession in a typical karst region in Southwest China. *Sci. Total Environ.* **2015**, *521*, 52–58. [\[CrossRef\]](#)
- Xiao, K.C.; He, T.G.; Chen, H.; Peng, W.X.; Song, T.Q.; Wang, K.L.; Li, D.J. Impacts of vegetation restoration strategies on soil organic carbon and nitrogen dynamics in a karst area, southwest China. *Ecol. Eng.* **2017**, *101*, 247–254. [\[CrossRef\]](#)
- Huang, C.J. Main vegetation types and distribution characteristics in Yuntai Mountain, Shibing, Guizhou province of China. *Guizhou For. Sci. Technol.* **1995**, *23*, 26–30.
- Luo, X.J.; Li, Q.M.; Feng, Y.C.; Wang, L.H.; Jiang, Y.L. Biodiversity and floristic characteristics of orchids in Dashahe Nature Reserve, Daozhen, Guizhou province of China. *Guizhou For. Sci. Technol.* **2013**, *41*, 19–23.
- Dong, M. Plant clonal growth in heterogeneous habitats: Risk-spreading. *Chin. J. Plant Ecol.* **1996**, *6*, 543–548.
- Six, J.; Conant, R.T.; Paul, E.A.; Paustian, K. Stabilization mechanisms of soil organic matter: Implications for C-saturation of soils. *Plant Soil* **2002**, *241*, 155–176. [\[CrossRef\]](#)
- Bao, S.D. *Soil Agrochemical Analysis*, 3rd ed.; China Agriculture Press: Nanjing, China, 2001; pp. 3–109.

30. Guan, S.Y. *Soil Enzymes and Research Methods*; Agricultural Press: Beijing, China, 1986; pp. 294–297.
31. Zhu, X.N. *R Language*; Renmin University of Chinese Press: Beijing, China, 2018; pp. 1–352.
32. Wang, C.Q.; Xue, L.; Jiao, R.Z. Soil organic carbon fractions, C-cycling associated hydrolytic enzymes, and microbial carbon metabolism vary with stand age in *Cunninghamia lanceolata* (Lamb.) Hook plantations. *For. Ecol. Manag.* **2021**, *48*, 482–496. [[CrossRef](#)]
33. Wu, Y.N.; Yu, L.F.; Zhang, L.M.; Liu, N.; Yan, L.B. Characteristics and influencing factors of soil carbon pool during vegetation restoration in Karst Plateau. *Ecol. Environ. Sci.* **2020**, *29*, 1935–1942. [[CrossRef](#)]
34. Ge, T.D.; Yuan, H.Z.; Zhu, H.H.; Wu, X.H.; Nie, S.A.; Liu, C.; Tong, C.L.; Wu, J.S.; Brookes, P. Biological carbon assimilation and dynamics in a flooded rice-soil system. *Soil Biol. Biochem.* **2012**, *48*, 39–49. [[CrossRef](#)]
35. Raich, J.W.; Schlesinger, W.H. The global carbon dioxide flux in soil respiration and its relationship to vegetation and climate. *Tellus* **1992**, *44B*, 81–99. [[CrossRef](#)]
36. Elipe, B.; Carlos, G.; Noah, F.; David, J.E.; Matthew, A.B.; Sebastián, A.; Fernando, D.A.; Asmeret, A.B.; Nick, A.C.; Antonio, G.; et al. Global ecological predictors of the soil priming effect. *Nat. Commun.* **2019**, *10*, 3481.
37. Zhang, L.M.; Xu, M.G.; Lou, Y.L.; Wang, X.L.; Qing, S.; Jiang, T.M.; Li, Z.F. Changes in Yellow paddy soil organic carbon fractions under long-term fertilization. *Sci. Agric. Sin.* **2014**, *47*, 3817–3825. [[CrossRef](#)]
38. Chen, Z.M.; Wang, H.Y.; Liu, X.W.; Zhao, X.L.; Lu, D.J.; Zhou, J.M.; Li, C.Z. Changes in soil microbial community and organic carbon fractions under short-term straw return in a rice-wheat cropping system. *Soil Tillage Res.* **2017**, *16*, 121–127. [[CrossRef](#)]
39. Lan, L.Y.; Yang, W.Q.; Wu, F.Z.; Liu, Y.W.; Guo, C.H.; Zhan, Y.; Tan, B. Effects of soil fauna on microbial community during litter decomposition of *populus simonii* and *fargesia spathacea* in the subalpine forest of western Sichuan, China. *Chin. J. Appl. Ecol.* **2019**, *30*, 2983–2991. [[CrossRef](#)]
40. Fontaine, S.; Mariotti, A.; Abbadie, L. The priming effect of organic matter: A question of microbial competition. *Soil Biol. Biochem.* **2003**, *35*, 837–843. [[CrossRef](#)]
41. Elliott, E.T.; Paustian, K.; Frey, S.D. Modeling the Measurable or Measuring the Modelable: A Hierarchical Approach to Isolating Meaningful Soil Organic Matter Fractionations. In *Evaluation of Soil Organic Matter Models*; Nato Asiseries; Springer: Berlin/Heidelberg, Germany, 1996; Volume 2, pp. 161–179.
42. Soh, S.; Makoto, S.; Antoine, D.M.Z.; Haruo, T.; Takashi, K.; Shinya, F. Forest understories controlled the soil organic carbon stock during the fallow period in African tropical forest: A <sup>13</sup>C analysis. *Sci. Rep.* **2019**, *9*, 9835–9843. [[CrossRef](#)]
43. Callesen, I.; Liski, J.; Raulund-Rasmussen, K.; Olsson, M.T.; Tau-Strand, L.V.; Westman, C.J. Soil carbon stores in Nordic well-drained forest soils—Relationships with climate and texture class. *Glob. Chang. Biol.* **2003**, *9*, 358–370. [[CrossRef](#)]
44. Wiesmeier, M.; Jörg, P.; Frauke, B.; Peter, S.; Uwe, G.; Edzard, H.; Arthur, R.; Bernd, S.; Margit, V.L.; Ingrid, K.K. Storage and drivers of organic carbon in forest soils of southeast Germany (Bavaria)-Implications for carbon sequestration. *For. Ecol. Manag.* **2013**, *295*, 162–172. [[CrossRef](#)]
45. Guan, J.H.; Deng, L.; Zhang, J.G.; He, Q.Y.; Shi, W.Y.; Li, G.Q.; Du, S. Soil organic carbon density and its driving factors in forest ecosystems across a northwestern province in China. *Geoderma* **2019**, *352*, 1–12. [[CrossRef](#)]
46. Schuman, G.E.; Janzen, H.H.; Herrick, J.E. Soil carbon dynamics and potential carbon sequestration by rangelands. *Environ. Pollut.* **2002**, *116*, 391–396. [[CrossRef](#)]
47. Merabtene, M.D.; Faraoun, F.; Mlih, R.; Riad, D.; Ali, L.; Roland, B. Forest Soil Organic Carbon Stocks of Tessala Mount in North-West Algeria-Preliminary Estimates. *Front. Environ. Sci.* **2021**, *120*, 125–138. [[CrossRef](#)]
48. Xu, J.H.; Gao, L.; Sun, Y.; Cui, X.Y. Distribution of mineral-bonded organic carbon and black carbon in forest soils of great Xing'an mountains, China and carbon sequestration potential of the soils. *Acta Pedol. Sin.* **2018**, *55*, 236–246. [[CrossRef](#)]
49. Zhang, Q. *Soil Carbon Distribution Characteristics and Carbon Sequestration Potential Estimation of Highway Shelterbelt in Taklimakan Desert*; Northwest Agricultural & Forest University: Shanxi, China, 2019.
50. Bertrand, I.; Delfosse, O.; Mary, B. Carbon and nitrogen mineralization in acidic, limed and calcareous agricultural soils: Apparent and actual effects. *Soil Biol. Biochem.* **2007**, *39*, 276–288. [[CrossRef](#)]
51. Oren, A.; Steinberger, Y. Coping with artifacts induced by CaCO<sub>3</sub>-CO<sub>2</sub>-H<sub>2</sub>O equilibria in substrate utilization profiling of calcareous soils. *Soil Biol. Biochem.* **2008**, *40*, 2569–2577. [[CrossRef](#)]
52. Di, J.Y. *Characteristics and Driving Factors of Mineral Combined Organic Carbon Saturation Deficit in Typical Farmland Soils under Long-Term Fertilization*; Chinese Academy of Agricultural Sciences: Beijing, China, 2017.
53. Sun, Z.X.; Bai, H.Q.; Ye, H.C.; Zhuo, Z.Q.; Huang, W.J. Three-dimensional modelling of soil organic carbon density and carbon sequestration potential estimation in a dryland farming region of China. *J. Geogr. Sci.* **2021**, *31*, 1453–1468. [[CrossRef](#)]
54. Dray, R.; Gorham, E. Litter production in forest of the world. *Adv. Res.* **1964**, *2*, 101–157.
55. Wang, X.P.; Yang, X.; Yang, N.; Xin, X.J.; Qu, Y.B.; Zhao, L.X.; Gao, Y.B. Effects of litter diversity and composition on litter decomposition characteristics and soil microbial community. *Acta Ecol. Sin.* **2019**, *39*, 1–9. [[CrossRef](#)]
56. Hartley, I.P.; Gatnett, M.H.; Hopkins, D.W.; Fletcher, B.J.; Sloan, V.L.; Phoenix, G.K.; Wookey, P.A. A potential loss of carbon associated with greater plant growth in the European Arctic. *Nat. Clim. Chang.* **2012**, *12*, 875–879. [[CrossRef](#)]
57. Qin, Y.B.; Xin, Z.B.; Wang, D.M.; Xiao, Y.L. Soil organic carbon storage and its influencing factors in the riparian woodlands of a Chinese karst area. *Catena* **2017**, *15*, 21–29. [[CrossRef](#)]
58. Chen, J.; Sinsabaugh, R.L. Linking microbial functional gene abundance and soil extracellular enzyme activity: Implications for soil carbon dynamics. *Glob. Chang. Biol.* **2021**, *27*, 122–135. [[CrossRef](#)] [[PubMed](#)]

- 
59. Tian, Q.X.; He, H.B.; Cheng, W.X.; Zhen, B.; Wang, Y.; Zhang, X.D. Factors controlling soil organic carbon stability along a temperate forest altitudinal gradient. *Sci. Rep.* **2016**, *6*, 242–258. [[CrossRef](#)] [[PubMed](#)]
  60. Liu, X.X.; Luan, Y.N.; Dai, W.; Wang, B.; Dai, A. Factors affecting soil organic carbon in a *Phyllostachys edulis* forest. *J. For. Res.* **2019**, *30*, 1487–1494. [[CrossRef](#)]